IEEE Photonics Journal
An IEEE Photonics Society Publication

Open Access

Large-Area Printed Broadband Membrane Reflectors by Laser Interference Lithography

Volume 5, Number 1, February 2013

Jung-Hun Seo, Student Member, IEEE
Jungho Park
Deyin Zhao
Hongjun Yang, Member, IEEE
Weidong Zhou, Senior Member, IEEE
Byeong-Kwon Ju, Member, IEEE
Zhenqiang Ma, Member, IEEE

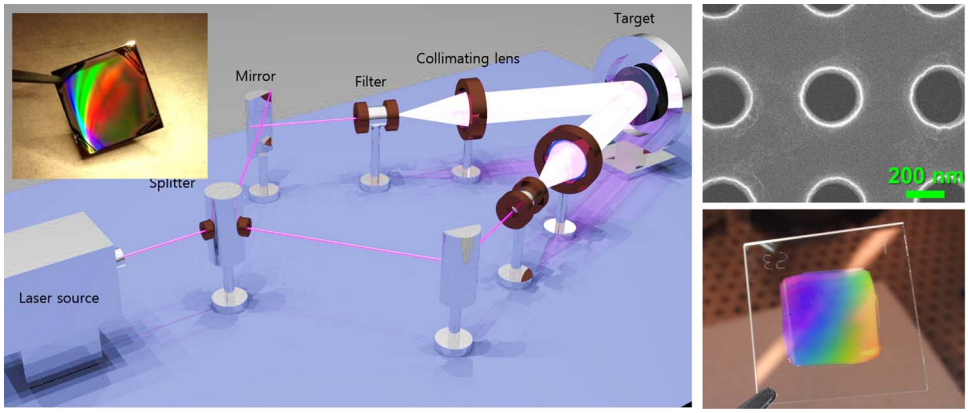

DOI: 10.1109/JPHOT.2012.2236545
1943-0655/$31.00 ©2013 IEEE

IEEE photonics SOCIETY

IEEE

Large-Area Printed Broadband Membrane Reflectors by Laser Interference Lithography

Jung-Hun Seo,[1] *Student Member, IEEE*, Jungho Park,[2] Deyin Zhao,[3] Hongjun Yang,[3] *Member, IEEE*, Weidong Zhou,[3] *Senior Member, IEEE*, Byeong-Kwon Ju,[2] *Member, IEEE*, and Zhenqiang Ma,[1] *Member, IEEE*

[1]Department of Electrical and Computer Engineering, University of Wisconsin-Madison, WI 53706 USA
[2]Display and Nano System Laboratory, School of Engineering, Korea University, Seoul 136-713, Korea
[3]Department of Electrical Engineering, NanoFAB Center, University of Texas, Arlington, TX 76019 USA

DOI: 10.1109/JPHOT.2012.2236545

Manuscript received October 28, 2012; revised December 17, 2012; accepted December 20, 2012. Date of current version February 4, 2013. These authors contributed equally to this work. This work was supported in part by the U.S. AFOSR under Grants FA9550-091-0482, FA9550-08-1-0337, and FA9550-11-C-0026 and in part by the Ministry of Knowledge Economy (MKE, Korea) through the IT R&D Infrastructure Program supervised by the NIPA (NIPA-2011-(B1110-1101-0002) and Grant No. 10041416). The program manager at AFOSR is Dr. Gernot Pomrenke. Authors J.-H. Seo, J. Park, D. Zhao, and H. Yang contributed equally to this work. Corresponding author: W. Zhou, B.-K. Ju, and Z. Ma (e-mail: bkju@korea.ac.kr; wzhou@uta.edu; mazq@engr.wisc.edu).

Abstract: We report here large-area broadband photonic crystal membrane reflectors (MRs) on glass substrates based on laser interference lithography (LIL) patterning and elastic stamp membrane transfer printing techniques. High-reflectivity broadband MRs on glass were realized with measured reflectivity of 95% around 1300 nm and a bandwidth of about 100 nm. Large-area nanopattern uniformity was experimentally verified with measured reflectivity from multiple locations of the large-area MRs. The work could lead to fabrication of the large-area high-performance MR at low cost with high throughput. The reflectors can be used in many types of optoelectronic and photonic devices.

Index Terms: Broadband membrane reflectors (MRs), transfer printing, silicon nanomembrane, laser interference lithography (LIL).

1. Introduction

Surface normal ultracompact broadband reflectors (BBRs) are considered as one of key components in optoelectronics applications such as microcavities, lasers, photodetectors, solar cells, sensors, reconfigurable photonics, etc. [1]–[4]. To create nanometer-sized patterns needed for these applications, conventional techniques such as nanoimprinting [5], [6], electron beam lithography [7], [8], and focused ion beam patterning [9] have been widely used. Many of these approaches involve a slow process and are not cost effective.

The laser interference lithography (LIL) technique offers one of the most promising approaches to the formation of large-area nanoscale patterns with high throughput and potentially at low cost [10], [11]. Although LIL has the limitation that it can only fabricate periodic patterns, it is an attractive alternative to conventional methods for applications in which periodic patterns are desirable, with examples including X-ray transmission gratings [12], photonic crystals [13], [14], and submicrometric sieves. [15] With this point of view, fabrication of periodic nanostructures with LIL suggests the easiest method to achieve large-size BBRs without losing performance aspect. In this

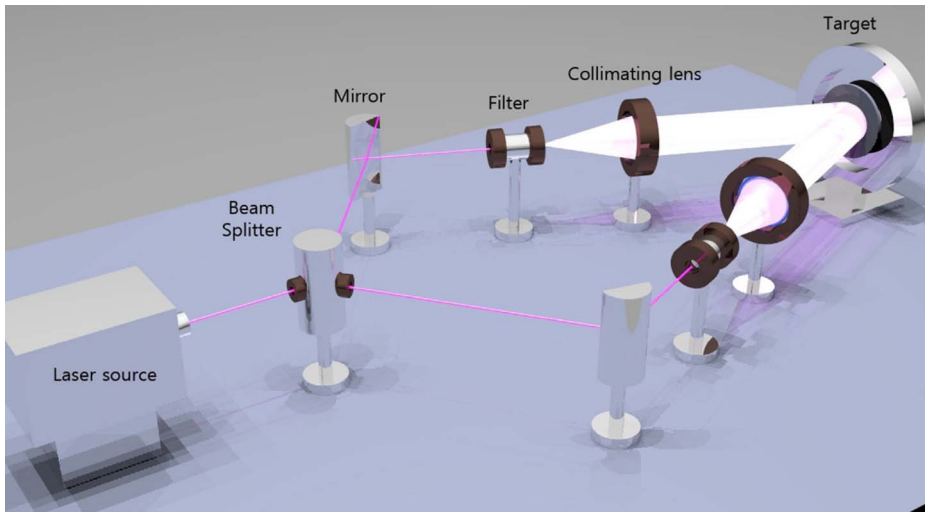

Fig. 1. Illustration of the LIL system setup. The laser source is a frequency-doubled argon-ion laser with a wavelength of 257 nm and an output power of 0.16 mW/cm^2.

paper, 4 cm^2 (2 cm $\times$ 2 cm)-sized single-layer membrane reflectors (MRs) for BBR were demonstrated based on a two-dimensional photonic crystal slab (2-D PCS) structure using the LIL patterning technique on a SOI wafer. Based on a transfer printing technique, the large-area MRs on glass were also realized.

2. Experiment

The MR fabrication process involves the patterning of photoresist by LIL on a SOI wafer that has a 340-nm-thick single-crystal silicon layer on top of a 2-μm buried oxide (BOX) layer. Adhesion layer was coated (HMDS : PGMEA $= 1 : 4$) before the photoresist (AR-N4240, mixed with Thinner AR 300-12 at a ratio 2 : 1) was spun coated onto the wafer, yielding a resist thickness of 400 nm. The samples were then exposed in a Lloyd's mirror interferometer [16], schematically shown in Fig. 1. The laser used for exposure is a frequency-doubled argon-ion laser with a wavelength of 257 nm and an output power of 0.16 mW/cm^2. The desired laser power was set by an optical power energy meter (Newport, 1936-C). The exposure was initiated with the sample loaded. The light is directed through a spatial filter, consisting of a focusing distribution of the initial laser beam of approximately 0.15 mm. The focal length is 3.4 mm, and the distance between the spatial filter and the sample holder is around 1.2 m. For our setup, the typical exposure time is 140 s. To create photoresist patterns with a square symmetry, two exposures by a rotation of 90° in between are applied. The periodicity, i.e., P of the resist pattern (pitch size) is determined by [17]

$$P = \frac{\lambda}{2 \cdot \sin\theta} \tag{1}$$

where λ is the wavelength of the laser used, and θ is the incident angle of the laser beam toward the specimen. Two beams are used: one travels directly to the specimen, and the other is reflected onto the specimen by a mirror. These two beams form an interference pattern on the specimen [11], [18]. Identical procedures were performed for further case studies in order to explore the effects of the critical factors, namely, the exposure dosage, the half angle between the two incident beams, and the beam power. A single exposure can generate a 1-D line pattern. Two-dimensional dot/hole patterns were generated from a successive exposure with 90° rotation of the sample. A total dosage of 0.16 mW/cm^2 $\times$ 140 s for dots (and 70 s $\times$ 2 times for holes) was used. In addition, a hole pattern array of 264-nm diameter and center-to-center pitch of 610 nm were realized. A dry etching procedure on the top Si with the photoresist as etching mask was followed on a SOI substrate, followed

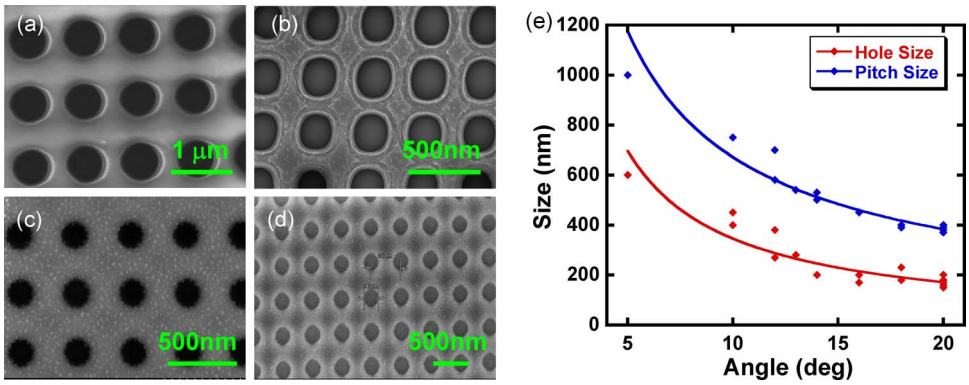

Fig. 2. (a)–(d) SEM images of transferred Si NM on glass substrate with light incident angles of 5°, 10°, 15°, and 20°, respectively. (e) Measured hole and pitch sizes as a function of the LIL angle.

by the selective undercut etching of the BOX layer by immersing the sample in hydrofluoric acid (HF). The released patterned top Si layer is referred to as Si membrane reflector (Si-MR).

The Si-MRs were then picked up and transfer printed to a glass substrate by employing a polydimethylsiloxane (PDMS) stamp transfer printing technique without using any adhesive layer. [19] To successfully transfer the patterned Si nanomembrane (Si NM), the PDMS stamped was optimized such that its adhesion force is suitable for the large-area patterned structure during its picking-up and placing-down processes. The peeling-off (printing) speed was also carefully controlled to avoid any potential wrinkling and breakage of the Si-MR. After transfer, the sample was annealed at 220 °C for 180 s using RTA under nitrogen atmosphere in order to improve the bonding strength between the transferred Si-MR and the glass substrate.

3. Results and Discussion

In order to optimize the LIL process conditions for the formation of circular air hole patterns, LIL angle tests were performed by changing the incident light angle toward the specimen using a mirror. When the incident angle was changed, other parameters such as exposure dosage and beam power were fixed. Scanning electron microscope (SEM) images in Fig. 2(a)–(d) show various photoresist patterns under different LIL angles. As the laser beam incident angle was increased from 5° to 20°, the hole pattern shape changes from slightly horizontal oval shape [see Fig. 2(a)] to circular shape and then to slightly vertical oval shape [see Fig. 2(d)]. At 15° incident angle [see Fig. 2(c)], a nearly perfect circular shape was obtained. It is noted that the shape of the nanopatterns is also affected by photoresist thickness, since the photoresist thickness is related to laser exposure. Besides the hole shape, the hole size and pitch size also change with the beam incident angle, as shown in Fig. 2(e), which is also expected based on (1). The pitch distance for 10°, 15°, and 20° can be calculated as 747, 497, and 375 nm, respectively. Therefore, controlling the LIL angle with optimal photoresist thickness is critical in order to form the desired nanopatterned MRs.

The nanomembrane area that can be patterned with LIL is also related to the beam incident angle, which decides the size of area where interference can happen. Using our setup, a 2.5 cm × 2.5 cm area can be uniformly patterned using 10° of LIL angle. Using 20° LIL angle, a 5 cm × 5 cm area can be uniformly patterned. Both hole and pitch size became saturated beyond 20° of LIL angle, which is limited by the wavelength of the laser source and the thickness of the photoresist. Since the LIL uses the interference of laser beams, laser light can be reflected more or less by the reflectivity of the substrate. To investigate the relationship between the reflectivity of the substrate and the size of the hole pattern, LIL patterning was carried out on 500-μm-thick bare glass, 200-nm-thick aluminum (Al)-coated glass, and SOI substrate under same lithography conditions. As shown in Fig. 3, since the photoresist thickness and the incident laser angle are identical for the three samples, the diameter and the pitch of patterned holes are solely influenced by the reflectivity of

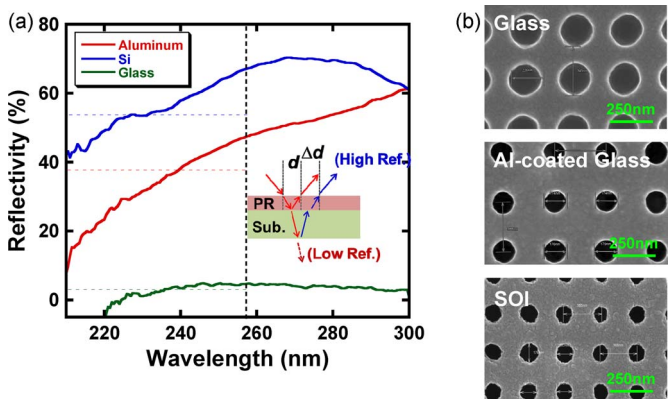

Fig. 3. (a) Measured reflectivity of LIL-patterned photoresist on various substrates in the wavelength range from 200 to 300 nm. The dashed vertical line is 257-nm wavelength. The inset shows the schematic of laser beam paths. (b) SEM images after finishing LIL on photoresist on bare glass, Al-coated glass, and silicon substrate, respectively.

each substrate. At 257-nm wavelength, Fig. 3(a) shows the measured reflectivity of 5%, 45%, and 65% for bare glass, Al-coated glass, and SOI substrate, respectively. The corresponding SEM images of these patterned samples are shown in Fig. 3(b).

To explain the influence of the pattern sizes and pitch distances with respect to the reflectivity of the substrate, we can assume two paths of UV laser beams during exposure. The first path is the light going into the photoresist and being reflected by the interface between the photoresist and the substrate. Therefore, photoresist is exposed within a distance of "d," as shown in the inset in Fig. 3(a). The second path is the one going through the photoresist and some of the light further goes into the substrate and then reflected by the back surface of the substrate. In this case, the photoresist is exposed within a distance of "$d + \Delta d$," which makes the final exposed area bigger as described in Fig. 3(b). For the case of bare glass, the exposure occurs along with both the first and second path, due to the low substrate reflectivity (5%). As the reflectivity of the substrate increases, the effect of the second path "Δd" becomes more negligible; therefore, the hole size is reduced. As a result, for the case of 20° LIL angle, the hole size decreases from 226 nm to 174 nm and to 162 nm for the bare glass, Al-coated glass, and SOI substrate, respectively. The corresponding ratio between the hole size and the pitch distance decreases from 1 : 2.38 to 1 : 2.23 and 1 : 2.11 for the three samples, respectively. Since the ratio from the SOI substrate agrees well with the results shown in Fig. 2, the explanation is roughly verified.

For the fabrication of MR for reflectivity measurements, we used 15° LIL angle. The corresponding SEM images are shown in Fig. 4(a) and (b). The measured patterning dimensions are 240-nm hole size and 500-nm pitch distance. Shown in Fig. 4(c) and (d) are sample images of a 2 cm $\times$ 2 cm sized Si NM MR, transferred to a glass substrate. With the PDMS-assisted transfer printing process, large-area and high-quality NMs have been successfully transferred without any visible fractures.

The reflectivity of the MR was measured at normal incidence with a beam size of around 100 μm. The spectra are shown in Fig. 5, for the reflectors before transfer (on SOI) and after transfer (on glass), respectively. The reflections of these MRs at different locations are also tested, and the results are plotted together using different colors. As shown in Fig. 5(a), the MR peak reflectivity on SOI is as high as 95% around 1300-nm wavelength with good uniformity at different locations. The bandwidth is about 100 nm from 1250 to 1350 nm. Theoretically, $\sim$100% reflection can be achieved [7], which can be realized with further fabrication optimizations. The current nonuniformity of the reflectivity data could be due to possible vibration during the LIL patterning and/or unintentional change in pattern size caused by the particles in the air of the laser path of the LIL system. These issues can be addressed by improving the lithography environment. Nevertheless, we believe that this is the simplest and easiest method to fabricate large-size surface normal ultracompact broadband MRs.

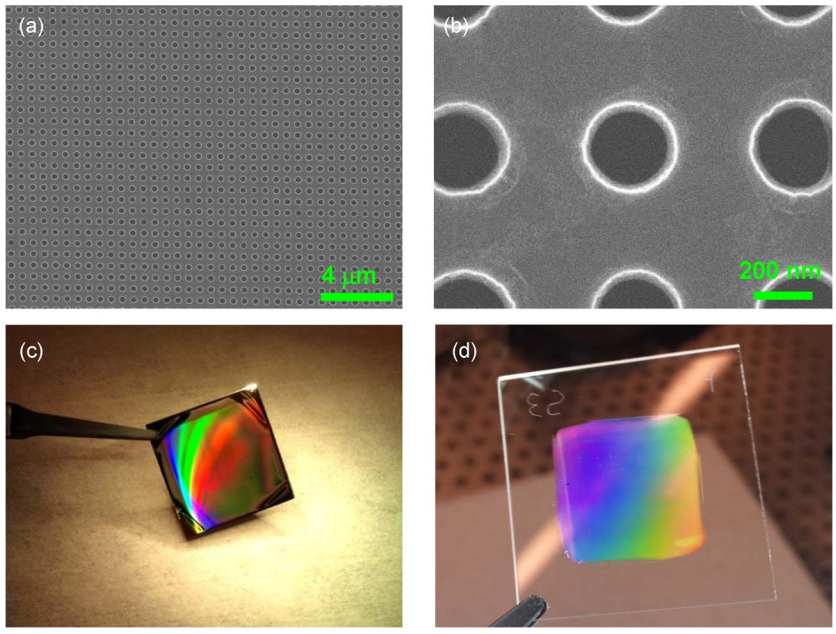

Fig. 4. (a) SEM image of the hole array pattern formed on a SOI substrate. (b) Zoomed-in image of (a). (c) Optical image of an LIL-patterned sample after dry etching of a top Si layer on SOI. (d) Optical image of a transferred Si NM MR on a glass substrate.

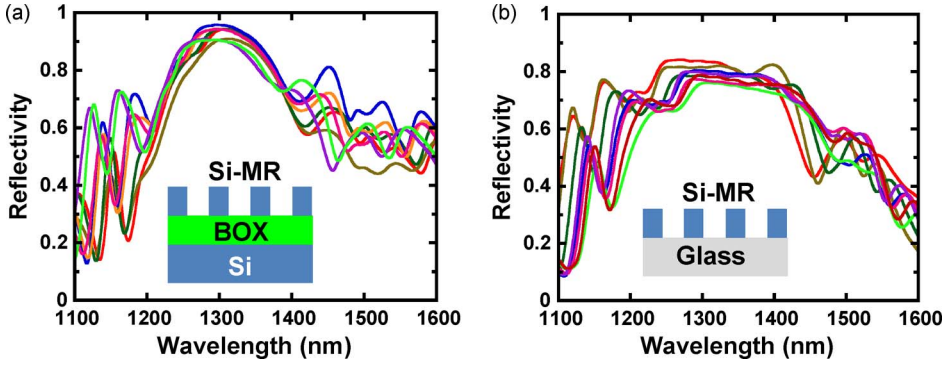

Fig. 5. Reflection spectra measured at different locations of the large-area Si-MR: (a) measured spectra of Si-MR on SOI wafer before undercutting of the BOX layer and (b) measured spectra of Si-MR after transferring onto a glass substrate.

For the MR on glass, as shown in Fig. 5(b), lower reflectivity was measured in comparison with that measured before transfer. The degradation might be caused mostly by the nonuniform size of holes and nonuniform center-to-center pitches as well as surface roughness of the glass substrate.

4. Conclusion

In conclusion, large-size broadband silicon nano-MRs on glass substrates were fabricated and demonstrated by using LIL patterning techniques and transfer printing techniques. Reflectivity as high as 95% around 1300-nm wavelength with a bandwidth of 100 nm was achieved. Higher reflection is expected under improved processing conditions. The work demonstrates a low-cost manufacturable approach to high-performance MRs with potential impact on many future opto-electronic and photonic applications.

References

[1] A. E. Willner, "Lasers: All mirrors are not created equal," *Nat. Photon.*, vol. 1, no. 2, pp. 87–88, Feb. 2007.

[2] M. C. Y. Huang, Y. Zhou, and C. J. Chang-Hasnain, "A surface-emitting laser incorporating a high-index-contrast subwavelength grating (vol 1, pg 119, 2007)," *Nat. Photon.*, vol. 1, no. 5, p. 297, May 2007.

[3] J. W. Leem, Y. M. Song, and J. S. Yu, "Broadband wide-angle antireflection enhancement in AZO/Si shell/core subwavelength grating structures with hydrophobic surface for Si-based solar cells," *Opt. Exp.*, vol. 19, no. S5, pp. A1155–A1164, Sep. 2011.

[4] H. Yang, D. Zhao, S. Chuwongin, J. H. Seo, W. Yang, Y. Shuai, J. Berggren, M. Hammar, Z. Ma, and W. Zhou, "Transfer-printed stacked nanomembrane lasers on silicon," *Nat. Photon.*, vol. 6, no. 9, pp. 617–620, Sep. 2012.

[5] M. Belotti, J. Torres, E. Roy, A. Pépin, Y. Chen, D. Gerace, L. C. Andreani, and M. Galli, "Replication of photonic crystals by soft ultraviolet-nanoimprint lithography," *J. Appl. Phys.*, vol. 99, no. 2, pp. 024309-1–024309-4, Jan. 2006.

[6] H. Schift, S. Park, B. Jung, C. G. Choi, C. S. Kee, S. P. Han, K. B. Yoon, and J. Gobrecht, "Fabrication of polymer photonic crystals using nanoimprint lithography," *Nanotechnology*, vol. 16, no. 5, pp. S261–S265, May 2005.

[7] H. Yang, D. Zhao, J. H. Seo, S. Chuwongin, S. Kim, J. A. Rogers, Z. Ma, and W. Zhou, "Broadband membrane reflectors on glass," *IEEE Photon. Technol. Lett.*, vol. 24, no. 6, pp. 476–478, Mar. 2012.

[8] H. Yang, S. Chuwongin, Z. Qiang, L. Chen, H. Pang, Z. Ma, and W. Zhou, "Resonance control of membrane reflectors with effective index engineering," *Appl. Phys. Lett.*, vol. 95, no. 2, pp. 023110-1–023110-3, Jul. 2009.

[9] N. Liu, A. Datta, C. Liu, and Y. Wang, "High-speed focused-ion-beam patterning for guiding the growth of anodic alumina nanochannel arrays," *Appl. Phys. Lett.*, vol. 82, no. 8, pp. 1281–1283, Feb. 2003.

[10] J. Choi, M. H. Chung, K. Y. Dong, E. M. Park, D. J. Ham, Y. Park, I. S. Song, J. J. Pak, and B. K. Ju, "Investigation on fabrication of nanoscale patterns using laser interference lithography," *J. Nanosci. Nanotechnol.*, vol. 11, no. 1, pp. 778–781, Jan. 2011.

[11] S. Brueck, "Optical and interferometric lithography—Nanotechnology enablers," *Proc. IEEE*, vol. 93, no. 10, pp. 1704–1721, Oct. 2005.

[12] M. L. Schattenburg, C. R. Canizares, D. Dewey, K. A. Flanagan, M. A. Hamnett, A. M. Levine, K. S. K. Lum, R. Manikkalingam, T. H. Markert, and H. I. Smith, "Transmission grating spectroscopy and the advanced X-ray astrophysics facility," *Opt. Eng.*, vol. 30, no. 10, pp. 1590–1600, Oct. 1991.

[13] I. B. Divliansky, A. Shishido, I. C. Khoo, T. S. Mayer, D. Pena, S. Nishimura, C. D. Keating, and T. E. Mallouk, "Fabrication of two-dimensional photonic crystals using interference lithography and electrodeposition of CdSe," *Appl. Phys. Lett.*, vol. 79, no. 21, pp. 3392–3394, Nov. 2001.

[14] M. Campbell, D. Sharp, M. Harrison, R. Denning, and A. Turberfield, "Fabrication of photonic crystals for the visible spectrum by holographic lithography," *Nature*, vol. 404, no. 6773, pp. 53–56, Mar. 2000.

[15] L. E. Gutierrez-Rivera and L. Cescato, "SU-8 submicrometric sieves recorded by UV interference lithography," *J. Micromech. Microeng.*, vol. 18, no. 11, p. 115 003, Nov. 2008.

[16] Q. Xie, M. Hong, H. Tan, G. Chen, L. Shi, and T. Chong, "Fabrication of nanostructures with laser interference lithography," *J. Alloys Comp.*, vol. 449, no. 1/2, pp. 261–264, Jan. 2008.

[17] R. Murillo, H. Van Wolferen, L. Abelmann, and J. Lodder, "Fabrication of patterned magnetic nanodots by laser interference lithography," *Microelectron. Eng.*, vol. 78/79, pp. 260–265, Mar. 2005, doi:10.1016/j.mee.2005.01.004. [Online]. Available: http://www.sciencedirect.com/science/article/pii/S0167931705000067

[18] J. de Boor, D. S. Kim, and V. Schmidt, "Sub-50 nm patterning by immersion interference lithography using a Littrow prism as a Lloyd's interferometer," *Opt. Lett.*, vol. 35, no. 20, pp. 3450–3452, Oct. 2010.

[19] M. A. Meitl, Z. T. Zhu, V. Kumar, K. J. Lee, X. Feng, Y. Y. Huang, I. Adesida, R. G. Nuzzo, and J. A. Rogers, "Transfer printing by kinetic control of adhesion to an elastomeric stamp," *Nat. Mater.*, vol. 5, no. 1, pp. 33–38, Jan. 2006.